β-Elemene Inhibits Proliferation of Non-Small-Cell Lung Cancer by Targeting ALDH3A1 to Regulate Metabolic Reprogramming

Yang Chen
The First Hospital of China Medical University: The First Affiliated Hospital of China Medical University
Xuena Li
The First Hospital of China Medical University: The First Affiliated Hospital of China Medical University
Xiaofang Che
The First Hospital of China Medical University: The First Affiliated Hospital of China Medical University
Yi Yang
China Medical University
Yao Diao
The First Hospital of China Medical University: The First Affiliated Hospital of China Medical University
Mingming Deng
The First Hospital of China Medical University: The First Affiliated Hospital of China Medical University
Kezuo Hou
The First Hospital of China Medical University: The First Affiliated Hospital of China Medical University
Xiujuan Qu
The First Hospital of China Medical University: The First Affiliated Hospital of China Medical University
Yunpeng Liu
The First Hospital of China Medical University: The First Affiliated Hospital of China Medical University
Yaming Li
The First Hospital of China Medical University: The First Affiliated Hospital of China Medical University
Ye Zhang
The First Affiliated Hospital of China Medical University
Xuejun Hu (xjhu@cmu.edu.cn)
the first hospital of china meidical university

Research

Keywords: Non–small-cell lung cancer (NSCLC), β-Elemene, Network pharmacology, ALDH3A1, HIF1α/LDHA signaling pathways

Posted Date: January 19th, 2021

DOI: https://doi.org/10.21203/rs.3.rs-147855/v1

Abstract

Background

Non-small cell lung cancer (NSCLC) is the most common cause of cancer-related death in the world. Although the improvement of treatment has significantly prolonged the survival of NSCLC patients, most patients still face recurrence because of drug resistance. Therefore, it is urgent to find more effective drugs to improve the NSCLC treatment and survival rate of patients.

Methods

Network pharmacology tools were comprehensive applied to analyze β-elemene and the anticancer effects of β-elemene were evaluated both in vitro and in vivo. What's more, the underlying mechanisms were investigated via metabolomics analysis, ^{18}FDG-micro-PET scan and molecular biology experiment.

Results

β-elemene exhibited potent inhibitory effects on NSCLC cells proliferation by alternating the cell cycle without significantly apoptosis in NSCLC cells. Mechanistically, we found that β-elemene regulating metabolic reprogramming of NSCLC via targeting Aldehyde Dehydrogenase 3 Family Member A1 (ALDH3A1). Subsequently, the metabolic reprogramming of NSCLC cells regulated by β-elemene lead to increased hydroxylation of α-ketoglutarate (α-KG), and degraded Hypoxia Inducible Factor1 Subunit Alpha (HIF1α), which cause accelerated reduction of aerobic glycolysis in NSCLC in vivo and vitro through facilitating HIF1α/LDHA pathway. Moreover, the reduction of aerobic glycolysis effect of β-elemene in vivo was confirmed by the reduced SUV values and the decreased expression of Ki-67 and HIF1α/LDHA pathway proteins in tumor tissues from xenograft mouse models.

Conclusion

β-Elemene exhibits strong metabolic reprogramming effects, glycolysis was suppressed while OXPHOS was increased in NSCLC cells via targeting ALDH3A1 and HIF1α/LDHA pathway, which provides a new theoretical basis for the clinical treatment of patients with NSCLC.

1. Background

NSCLC is the most frequent cause of cancer-related deaths worldwide[1]. Because the implementation of high-quality lung cancer screening still faces many challenges, 79% of lung cancers still are diagnosed as regional or distant disease[2]. There are a variety of treatments, including target therapy and immunotherapy which significantly improve the five-year survival rate of patients[3], most of them still

face treatment failure[4, 5]. Therefore, it is urgent to explore and optimize the treatment to gradually improve the poor 5-year survival rate of patients.

Traditional Chinese Medicine has long been indicated can suppress tumor progression[6]. The most recent study indicated that TCMs were more and more widely used in clinical cancer therapy[7]. β-elemene is a monomer compound extracted from the traditional Chinese medicine herb Curcuma wenyujin and has shown promising anticancer activity in a broad spectrum of tumors[8]. Mounting studies have reported that β-elemene can promote cell apoptosis in brain tumor and reverse the multi-drug resistance in gastric adenocarcinoma cells[9, 10]; β-elemene also can inhibit breast cancer metastasis by inhibiting pyruvate kinase M2 (PKM2) mediated glycosysis [11, 12]. In addition, β-elemene has also been reported to be able to inhibit the macrophages polarization from M2 to M1 and suppressed the development of lung cancer cells[13]. Therefore, β-elemene plays a crucial role in anti-tumor therapy. However, the hub target of β-elemene in cancer therapy is still largely unknown. In recent years, there has been an increasing interest in bioinformatics with the increased availability of genomic resources, and network pharmacology has already been widely used in targets discovery, especially in Chinese medicine (CM) formula[14, 15]. Therefore, network pharmacology and bioinformatics analysis will help to identify the targets of β-elemene and clarify its anti-tumor mechanism[16].

In this study, we identified ALDH3A1 was the hub target of β-elemene for the first time. We found that β-elemene could significantly suppress the proliferation of NSCLC cells in vivo and in vitro by inhibiting the expression of ALDH3A1, and the following HIF1α/LDHA pathway mediated glycolysis. As aerobic glycolysis plays a pivotal role in tumor development and drug resistance, while β-elemene has long been a great choice to suppress tumor progression after standard treatment fails. Overall, the study proposes that β-elemene is a promising drug used in combination with chemotherapy or other therapies in the treatment of early lung cancer.

2. Materials And Methods

2.1 Cell culture

NSCLC cell lines A549 and H1299 were purchased from the Academy of Military Medical Science (Beijing, China). A549 was cultured in DMEM/F-12 medium (Gibco, Carlsbad, CA), and the others were cultured in RPMI-1640 medium (Gibco, Carlsbad, CA) containing with 10% fetal bovine serum (FBS), penicillin (100U/mL) and streptomycin (100 mg/mL) at 37℃, in a humidified incubator with 5% CO_2. Cells were routinely passed every 2–3 days and all cells maintained in culture for a maximum 8 weeks.

2.2 Reagents and antibodies

β-Elemene (molecular formula of $C_{15}H_{24}$ and molecular weight of 204.35) for cell experiment purchased from Sigma-Aldrich (St. Louis, MO, USA), and the oral type was gifted from Jingang Pharmaceuticals (#081152, Dalian, China). Antibodies of HIF-1α (#3716S), LDHA (2012S)were obtained from Cell Signalling Technology (Danvers, MA, USA). Antibody of Cyclin B1 (166757), Cyclin D1 (8396), Cyclin

E,Actin (sc-47778), was purchased from Santa Cruz Biotechnology (Santa Cruz, CA, USA). Antibody GLUT1 (2646S) was purchased from NOVUS (USA) and antibody PFKL (55028-1-AP) was purchased from Proteintech. Anti-PDK1(ab226963) and Anti-PHD1 (ab113077) were purchased from Abcam. Anti-Ki67 antibody was purchased from Fuzhou Maixin Biological Technology (Fujian, China).

2.3 Cell proliferation assay

The proliferation assays in selected NSCLC cell lines were measured using a 3-(4,5Dimethylthiazolyl-2-yl)-2,5-diphenyltetrazolium bromide (MTT) assay. Firstly, A549 and H1299 cells were seeded at 3×10^3 cells/well in 96-well plates while HCC827 and PC9 cells were seeded at 4×10^3 cells/well in 96-well plates. After incubation for 24 h, the cells were treated with various concentrations of β-elemene for 24 or 48 h, Twenty microliter of MTT solution (5 mg/ml) was added to each well followed by 4 h incubation at 37 °C. The cell culture medium was removed and the cells were lysed in 200 μl dimethylsulphoxide (DMSO) and the results were measured using a microplate reader (Model 570, Bio-Rad Laboratories, Hercules, CA, USA).

We apply the method described in ref to detect cell proliferation. Briefly, the cells transfected with ALDH3A1-specific siRNAs (Si1 and Si2) and negative control siRNA (NC) for 4 days. The cell growth was determined using the CellTiter 96 Aqueous One Cell Proliferation Assay (Promega, Madison, WI). Percentage of net growth at day 4 (100%) relative to day 0 (0%) was calculated and the concentration of compound required to inhibit growth by 50% (GI50) determined. The assays were done in triplicate across different plates.

2.4 Colony-forming assay

A549 and H1299 cells were plated at 300 cells into each well of 12-well plates in the medium containing 10% FBS. Cells were incubated at 37℃ in 5% CO_2 for 3 days, after cell proliferation reaches the logarithmic growth phase, then cells were treated with multiple concentrations of β-elemene (20ug/ml and 30ug/ml). After 14 days, cells were stained by Wright–Giemsa. Finally, the number of colonies was counted by light microscopy.

2.5 The Edu assay

Selected NSCLC cells were seeded into 96-well plates (3000 cells per well). After incubation for 24 h, the cells were pretreated with β-elemene for 24 h or 48 h. Then 50 μM of 5-ethynyl2'-deoxyuridine (EdU, Ribobio, Guangzhou, China) was added to each well and the cells were incubated at 37 °C for 2 h before being fixed with 4% formaldehyde for 30 min and incubated with 2 mg/ml glycine for 5 min. After being washed with PBS for 3 times, the cells were reacted with 100μL of 1×Apollo reaction cocktail for 30 min. Afterwards, the 1×Hoechst 33342 (5 μg/mL) was used to stain the nuclei. Five representative fields of each insert were randomly counted under a microscope (Olympus, Tokyo, Japan) and analyzed statistically.

2.6 Flow cytometry analysis

The selected cells were cultured in 6-well plates and treated with or without different doses of β-elemene and then further incubated for 12 h or 24 h. Before the test, cells were incubated with 10μL phosphatidylinositol and 5μL Annexin V for 20 min protected from light for cell apoptosis. For cell cycle analysis, the cells were suspended in 70% ethanol, incubated at -20 °C for 2 h, and collected by centrifugation at 1500 rpm for 3 min. After removal of the ethanol, the cells were re-suspended in 300 μl PI staining solution and incubated for 30 min in dark. Then, the samples were evaluated by flow cytometry, and finally analyzed by Cell Quest software (USA) and modfit software.

2.7 Network pharmacology analysis

BATMAN-TCM (http://bionet.ncpsb.org/BATMAN-TCM) is the first tool for bioinformatics analysis for studying the molecular mechanism of TCM's by predicting potential targets for ingredients. The PubChem_CID / InChI of β-elemene (6918391) were entered as search queries. The following parameter settings were used: Target Prediction's Score cutoff was 20; Target Analysis's Adjusted P-value is less than 0.05. The PPI pairs of all the targets of β-elemene were analyzed using the online database STRING version 10.5 (http://string-db.org/). The pairs with combined scores > 0.4 were used for the PPI network construction, then the Cytoscape v.3.6.0 software was used to construct the network and analyze the interaction relationship of the proteins. Pathway enrichment analysis was performed using the clusterProfiler package[17].

2.8 Intracellular glucose uptake assay

First of all, A549 and H1299 cells were seeded into 96-well plates (3000 cells per well), after 24 h, treated with β-elemene, then incubate for another 24 h. Lastly, cultured in glucose-free medium overnight. After removal of the culture medium, the levels of intracellular glucose were assessed using a fluorescence-based glucose assay kit (BioVision) according to manufacturer's instructions.

2.9 Lactate Production Assay

Selected NSCLC cells were plated at 1×10^5 cells into each well of 6-well plates in the medium containing 10% FBS. Treat with different doses of β-elemene after 24 h and incubate for 4 hours. Then, the levels of lactate in the medium were quantitated with a lactate assay kit that is based on fluorescence activity (BioVision) according to manufacturer's instructions.

2.10 NADP+/NADPH, NAD^+/NADH Ratio and α-KG Assay

Selected NSCLC cells were plated at 1×10^5 cells into each well of 6-well plates in the medium containing 10% FBS. Treat with different doses of β-elemene after 24 h and incubate for 4 hours. Then, NADP+/NADPH, NAD+/NADH Ratio or α-KG levels in the cell lysates were determined using a fluorescence-based lactate assay kit (AAT Bioques for NADP+/NADPH, AAT BioquesforNAD$^+$/NADH Ratio, BioVision for α-KG) according to the manufacturers' instructions.

2.11 Intracellular PH assay

Dissolve Nigericin in 345 µL anhydrous DMSO to make a 20 mM solution. At the same time, dissolve Valinomycin in 225 µL anhydrous DMSO to make a 20 mM solution. Then, combine 100 µL of Nigericin and 100 µL of Valinomycin solutions to make a 1000× stock solution (10 mM each). Dilute 10 µL of this solution into 10 mL of the desired Intracellular pH Calibration Buffer to make a cell loading solution. Perform desired cellular experiment with pH-sensitive pHrodo™ dyes or conjugates. Washing cells 2× with Live Cell Imaging Solution (LCIS) (Cat. no. A14291DJ), replacing LCIS with the cell loading solution, and incubate at 37 °C for at least 5 minutes. Analyze the cells using the appropriate Ex/Em maxima.

2.12 ALDH3A1 enzymatic assay

ALDH3A1 was measured as previously described using 5 µg/ml of recombinant protein. Briefly, enzymatic activity was measured spectrophotometrically by the reduction of NAD + to NADH at A340 over 5 min in the presence of increasing concentrations of β-elemene or DMSO vehicle control. Assays were conducted in 50 mM sodium pyrophosphate buffer (pH 7.4) in the presence of 2.5 mM NAD^+ and 10 mM substrate and measured at 25 °C. Dose-response curve fits and EC50's were calculated using GraphPad Prism 7 software.

2.13 RNA and Lentivirus interference

ALDH3A1-specific siRNAs (Si1 and Si2) and negative control siRNA (NC) were prepared by ViewSolidBiotech (Beijing, China). The coding strand of human ALDH3A1Si1 was 5'-GGAACUCAGUGGUCCUCAATT-3', and that of ALDH3A1Si2 was 5'-UUGAGGACCACUGAGUUCCTT-3'. siRNAs were transfected into cells using Lipofectamine 2000 (Invitrogen) according to the manufacturer's protocol.Lentivirus construction of ALDH3A1 knockdown carrying green fluorescent protein (GFP) was designed and provided by Obio Technology Corp., Ltd. (Shanghai, China). A549 cells were transfected with the lentiviral vector according to the manufacturer's instructions. Control cells were transfected with empty vector carrying GFP. The ALDH3A1 knockdown cells were named Sh-ALDH3A1, and empty vector cells, named as Sh-NC, were used as control.

2.14 RNA isolation and qRT-PCR

Total RNA from the cultured cells was isolated with Trizol reagent (Invitrogen, Carlsbad, CA, USA) and the concentration of the total RNA was quantified by measuring the absorbance at 260 nm. All reagents for the reverse transcription (RT) were obtained from TaKaRa (Shiga, Japan). The PrimeScript™ RT Reagent Kit (Takara, Japan) was used for mRNA RT. Quantitative real-time PCR was performed using SYBR Premix Ex Taq II (TaKaRa) and measured in Applied Biosystems® 7500 Real-Time PCR Systems (Thermo Fisher Scientific, Waltham, MA, USA). The internal control used was 18S. The $2^{-\Delta\Delta Ct}$ method was used to calculate the fold change of the RNA expression of one sample compared to the calibration sample. The PCR primers used were as follows: ALDH3A1 forward: 5'- TGTTCTCCAGCAACGACAAGG-3'; ALDH3A1 reverse: 5'-GTGGGAATGTGAGCTGGAAC-3'; HIF-1α forward: 5'- TGTTCTCCAGCAACGACAAGG-3'; HIF-1α reverse: 5'-GTGGGAATGTGAGCTGGAAC-3'; GLUT1 forward: 5'- TGTTCTCCAGCAACGACAAGG-3'; Glut1 reverse: 5'-GTGGGAATGTGAGCTGGAAC-3'; PFKL forward: 5'- TGTTCTCCAGCAACGACAAGG-3'; PFKL

reverse: 5'-GTGGGAATGTGAGCTGGAAC-3'; LDHA forward: 5'- TGTTCTCCAGCAACGACAAGG-3'; LDHA reverse: 5'-GTGGGAATGTGAGCTGGAAC-3'; 18S forward: 5'- AGGGCAGAGAGTGCAAGGT-3'; 18S reverse: 5'-CGCCCGCCCGCTCCCAAGAT-3'.

2.15 Western blot analysis

For western-blotting in A549 and H1299 cell lines, the detailed method was described in ref. The cells were collected after treatment for indicated time and washed twice with cold PBS. Then cells were lysed in 1% Triton lysis buffer (50 mmol/L Tris-HCl, pH 7.4, 10 mmol/L EDTA, 100 mmol/L NaF, 150 mmol/L NaCl, 1% Triton X-100, 1 mmol/L PMSF 1 mmol/L Na3VO4 and 2 μg/mL aprotinin). After sonication and centrifugation, samples were quantified with the Lowry method. Next, all the protein samples were boiled at 95 °C for 5 min with 3× sampling buffer. After that, all the lysate samples were resolved by SDS polyacrylamide gel electrophoresis (SDS-PAGE) and followed by western blotting which means electronically transferred to polyvinylidene fluoride (PVDF) membranes. After blocking with 5% skim milk in TBST buffer (10 mM Tris-HCl pH 7.4, 150 mM NaCl, 0.1% Tween 20) at room temperature for 1 h, the blots were incubated with indicated antibodies shaking for 2 h, then overnight at 4 °C. Then the blots were washed four times with TBST buffer, and then incubated with secondary antibodies for 30 min at room temperature. After washing for another four times, the protein bands were detected with enhanced chemiluminescence reagent (SuperSignal Western Pico Chemiluminescent Substrate; Pierce, Rockford, IL, USA) and visualised with the Electrophoresis Gel Imaging Analysis System (DNR Bio-Imaging Systems, Jerusalem, Israel).

2.16 Xenograft studies

All in vivo experiments were performed in accordance with Institutional Review Board of China Medical University guidelines. Female 4–6 weeks old athymic BALB/c nude mice were purchased from Beijing Vital River Laboratory Animal Technology Co, Ltd. (animal experimental license no. SYXK2017-0033, Beijing, China). On the one hand, A549 cells (3×10^6) in 150 μl PBS were injected subcutaneously into the right scapular region of mice, On the other hand, A549 cells (3×10^6) expressing control shRNA or ALDH3A1 shRNA were s.c. injected into the dorsal flanks of 4-week-old female athymic BALB/c nude mice. After the average tumor size reached 150–200mm^3, animals were randomly divided into 2 groups, each containing six mice and were treated with vehicle only (Saline) which orally received 0.9% saline, β-elemene only (50 mg/kg by oral gavage once daily) for 10 days. Tumors were measured with a caliper every 2 days, so did body weights. Tumors' volume was calculated using the formula V = 1/2 ($width^2$ ×length) and the metabolic level of tumors were rely on Micro-PET scan. Mice were terminated by CO_2 inhalation when the tumor diameters reached 1.5 cm, according to the protocol filed with the Guidance of Institutional Animal Care and Use Committee of China Medical University.

2.17 Micro-PET scan

Firstly, the model mice were anesthetized by abdominal cavity. The volume of ^{18}FDG was not more than 0.1 ml. The activity, activity and measurement time were measured. ^{18}FDG was injected into tail vein. The injection time was recorded. The residual activity of syringe was measured. The residual activity and measurement time were recorded. After 30 minutes, the ^{18}FDG intake by mice was full, the model animals were transferred to the scanning bed and adjusted. The whole posture stretches its limbs, configures the micro-PET scanning (Metis-6) and related control software (Metis Console) and scanning.

2.18 ^{13}C metabolite labeling and quantification of energy metabolites

To extracting metabolites, first of all, add 200μL of pre-cooled ultrapure water to 60 mg of each mouse tumor tissue perform MP homogenization, followed by 800μL of pre-cooled methanol/acetonitrile(1:1, v/v).Samples were separated using an Agilent 1290 Infinity LC Ultra High Performance Liquid Chromatography System. Mass spectrometry in negative ion mode using a 5500 QTRAP mass spectrometer (AB SCIEX) analysis. Finally, the peak area and retention time were extracted using Multi quant software. The quality standard corrects the retention time and performs metabolite identification.

2.19 Immunohistochemistry

Tumors were formalin-fixed, paraffin-embedded and prepared as described in our previous study for staining with haematoxylin and eosin. The immunohistochemical antibodies ALDH3A1, HIF-1α, GLUT1, LDHA, Actin and Ki67 have been described already. The staining was evaluated by scanning the entire tissue specimen under low magnification (×10) and confirmed under high magnification (×20 and ×40). The protein expression was visualised and classified based on the percentage of positive cells and the intensity of staining. From each section, five visual fields were randomly selected. The degree of protein expression was based on the percentage of positive cells and the intensity of staining. Staining intensity was scored as 0 (no staining), 1 (low staining), 2 (intermediate staining), and 3 (high staining). For the staining area, ≤ 5%, 5–25%, 26–50, 51–75% >75% were recorded as 0, 1, 2, 3 and 4 points, respectively. Histological score = staining intensity× staining area. A score 0 was classified as negative (−), 1–4 points as weakly positive (+), 6–12 points as a strong positive (++). Final scores were assigned by two independent pathologists.

2.20 Statistical analysis

All the presented data were verified by three separate experiments, and are expressed as the means ± standard deviation (SD). Differences between groups were calculated by Student's two-tailed t-test. All analyses were calculated using GraphPad Prism software or R. $P < 0.01$ and $P < 0.05$ were considered statistically significant.

3. Results

3.1 β-Elemene inhibited NSCLC proliferation by alternating the cell cycle

We identified the inhibition effect of β-elemene in NSCLC cells proliferation, and the results revealed that β-elemene inhibited the proliferation of the A549 and H1299 NSCLC cells significantly, the IC_{50} values of β-elemene in A549 cells was 27.4 ± 0.60 ug/ml and 22.42 ± 0.89 ug/ml, and in H1299 cells was 27.47 ± 1.71 ug/ml and 23.07 ± 1.345 ug/ml; the effect was dose depended while the time dependence was not so obviously (Fig. 1A).The colony-forming assay showed 25 ug/ml and a higher dose 40ug/ml of β-elemene inhibited the proliferation of the A549 and H1299 NSCLC cells considerably (Fig. 1B). We further examined DNA replication in early phase using EdU assays, And the results showed β-elemene could affect DNA replication significantly after cells were incubation in with β-elemene for 12 hours, and this effect was enhanced by increasing the dose (Fig. 1C-D). β-Elemene treatment increased the G0/G1 cell cycle subpopulation cells and reduced the subpopulation of G2/M and S phase cells. This effect was increased when extending incubation time to 24 hours (Fig. 1E). but there were no obvious apoptotic cells (Figure S1A). Consistently, β-elemene treatment down regulated Cyclin A, Cyclin D1, Cyclin E in both A549 and H1299 cells (Fig. 1F). β-Elemene can also significantly inhibit tumor proliferation in the xenograft model (Fig. 1G). We did not observe treatment-related deaths or body weight loss in mice treated with β-elemene and the tumor-inhibiting capability is 61.6% (Fig. 1H).

3.2 β-Elemene regulated metabolic reprogramming

The network analyses via BATMAN-TCM showed the main KEGG pathway β-elemene work is metabolic pathway (Fig. 2A). There were only 31 proteins with a score higher than 50 (Table 1). So, we used these proteins to construct a protein-protein interaction (PPI) network with STRING (Figure S2A), and pathway enrichment analyses were performed via KEGG. The top 4 core pathways are simultaneously related to metabolic including Tyrosine metabolism, Metabolic pathways, Drug metabolism and Glycolysis/Gluconeogenesis (Fig. 2B). Furthermore, to identify whether β-elemene could regulate metabolism reprogramming, we established A549 xenograft model in nude mice (Fig. 2C). The ^{18}FDG micro-PET scan revealed that after treating with β-elemene, the SUV values of the tumors in vivo were significantly down regulated (Fig. 2D).

LC-MS analysis was performed on whole-tumor extracts, in order to dissect metabolic alterations,^{13}C metabolite labeling and quantification showed there were some heterogeneity between the treatment and control group, but we could still see some significant differences (Fig. 3A). In the treatment group, glucose, pyruvate, lactate, ATP and NAD/NADH ratio, which were produced during glycolysis, were obviously decreased, while the production of TCA cycle such as citrate and α-KG were increased significantly. The NADP/NADPH ratio and fumarate had an increase trend but $P > 0.05$ (Fig. 3B-C). We further used NSCLC cells to identify some of the metabolites in vitro. The in vitro and in vivo results were consistent, and showed β-elemene significantly decreased the glucose, lactate and NAD^+/NADH ratio in

cells, while increased α-KG and NADP/NADPH ratio. We also observed that β-elemene can significantly decrease the PH intracellular because of the NAD/NADH ratio changed in cells (Fig. 3D).

3.3 β-Elemene targeted ALDH3A1 to inhibit NSCLC cell proliferation

We intersected the genes in the top four enriched KEGG pathways to obtain 9 key role proteins, including ALDH1A3, ADH1A, ADH1B, ALDH3B2, ADH7, ALDH3A1, ADH5, ADH4, ADH6 (Fig. 4A). Firstly, we analyze the correlation between these molecules (Figure S3A-B). Then we evaluated the expression of these proteins in NSCLC patients and normal patients with the data from TCGA and GTEx. ALDH3A1 was the only one to have significant difference between cancer and normal tissue, while ALDH3B2 only had significant difference between cancer and normal tissue in LUSC (Fig. 4B). On the other hand, the correlation between ALDH3A1 and glycolysis related molecules SLC2A1 was particularly evident with R = 0.63, while the correlation between ALDH3B2 and SLC2A1 was not considerably noticeable with R = 0.36 (Fig. 4C).

The effect of ALDH3A1 on cell proliferation was assessed using NSCLC cells treated with β-elemene, siALDH3A1 or ALDH3A1 inhibitor DEAB individually or together. After treatment with different doses of β-elemene for 24 h, both cell lines exhibited suppressed ALDH3A1 mRNA and protein expression (Fig. 4D-E). The enzyme activation of ALDH3A1 was also dose-dependent down regulated by β-elemene in both cell lines (Fig. 4F). After comparing the knockdown effect of Si-1, Si-2 and Si-3, Si-1 and Si-2 displayed higher effect both at the mRNA and protein levels (Figure S3C-D). We next applied lentivirus Sh-ALDH3A1 to knockdown ALDH3A1, and the knockdown effect of Sh-ALDH3A1 both at the mRNA and protein levels were higher than 50% (Figure S3E-F). Si-1, Si-2, Sh-ALDH3A1 and DEAB successfully suppressed ALDH3A1 and inhibited NSCLC cells proliferation (Fig. 4G). The Sh-ALDH3A1 was effective alone identified via colony forming assays, and its effect was enhanced upon co-administration of DEAB (Fig. 4H). β-elemene could suppressed DNA replication obviously, and this effect was enhanced by the addition of β-elemene in both NSCLC cells (Fig. 4I-J).

3.4 ALDH3A1 control HIF1α-Mediated NSCLC glycolysis in vivo and in vitro

We could see the metabolites in TCA cycle increased while the production of ATP was obviously decreased after β-elemene treatment (Fig. 3B-C), which was the main energy source. We next examined whether the loss of ALDH3A1 influenced tumor metabolism and possible mechanism.^{18}FDG micro-PET imaging of mice with Sh-NC tumors in the left and Sh-ALDH3A1 tumors in the right, which had a similar metabolic index (Fig. 5A), showed considerably lower SUV values in the right tumors indicating a potential decrease in glucose uptake in Sh-ALDH3A1 tumors, and this effect was significantly enhanced upon β-elemene treatment (Fig. 5B-C).The metabolites analysis showed glucose uptake, production of lactate and NAD+/NADH ratio were significantly decreased, the cytosolic levels of NAD + and the NAD+/NADH ratio were major role to sustain glycolytic flux[18],while the α-KG was considerably up

regulated and these effects were simultaneously enhanced upon β-elemene treatment (Fig. 5D).These reminded us that α-KG is used as the electron donor of PHDs for prolyl hydroxylation and degradation of HIF1α[19]. Indeed, silencing of ALDH3A1 suppressed HIF1α,and also decreased the expression of a number of transcriptional targets of HIF1α, which including GLUT1, PDK1, LDHA, and PFKL in A549 NSCLC cells. Consistently, overexpression of ALDH3A1 increased HIF1α and also up-regulated the expression of GLUT1, PDK1, LDHA, and PFKL in H1299 NSCLC cells (Fig. 5E-F). This impact suggested that the regulatory effect of ALDH3A1 on glycolysis are mediated by HIF1α. Furthermore, treatment with Octyl-α-KG, the cell-permeable α-KG, similar to knockdown ALDH3A1 in A549 and reversed the effect of overexpression of ALDH3A1 in H1299 (Fig. 5G-H). Taken together, these results indicate that ALDH3A1 suppress NSCLC cell glycolysis via downregulating HIF1α and downstream signaling pathways.

3.5 ALDH3A1 down-regulation by β-Elemene induces HIF1α/LDHA pathway inhibited

Combinatorial treatment with β-elemene and Sh-ALDH3A1 enhanced the effect of Sh-ALDH3A1 significantly to inhibiting the expression of HIF1α and substantially downregulated GLUT1, LDHA, and PFKL in A549 and H1299 cells (Fig. 6A-B, Figure S4a). The down-regulation of Cyclin A, Cyclin D1, Cyclin E in both A549 and H1299 cells was significantly enhanced upon β-elemene treatment (Fig. 6C). We next identified the HIF1α/LDHA pathway and cell cycle related proteins in whole-tumor extracted proteins, and the result was consistent with that in A549 and H1299 cells (Fig. 6D-E).

Finally, we identified the functional significance of ALDH3A1 and β-elemene in vivo. ALDH3A1 knockdown and β-elemene inhibited the growth of A549 cells transfected with lentivirus xenografts in nude mice and we did not observe other side effects, body weight loss or treatment-related mortality in the mice treated with β-elemene and lentiviral (Fig. 7A-E). Immunohistochemistry assay showed a significant decrease in Ki-67, ALDH3A1, HIF1α, GLUT1, LDHA, and PFKL in the β-elemene, Sh-ALDH3A1 group and the effect was enhanced upon combinatorial treatment (Fig. 7F). Therefore, these results indicated that the tumor suppressive effect of β-elemene is achieved by targeting ALDH3A1 to inhibit the HIF1α/LDHA pathway.

4. Discussion

In this study, we found that β-elemene inhibited NSCLC proliferation by targeting ALDH3A1 to control the NAD/NADH ratio, reprogramming glycolysis and OXPHOS balance via suppressing HIF1α/LDHA pathway in vivo and in vitro. Our report proved the great potential of β-elemene in future tumor treatment which had not been deeply studied before.

Although multiple studies have explored the anti-tumor mechanism of β-elemene before, the direct target of β-elemene has not yet been determined. Recently, Y.Pan et al found that β-elemene can inhibit the metastasis of breast cancer via suppressing glycolysis[11], which analyzed by PharmMapper[20, 21], the network pharmacology tool which based on pharmacophore model to analyze the action effects. In

addition to the pharmacophore there are many other mechanisms. Unlike previous studies, we identified ALDH3A1 as the key target of β-elemene via BATMAN-TCM and bioinformatics methods[15, 22]. Compared with PharmMapper, BATMAN-TCM integrates the known interactions in DrugBank, TTD and KEGG databases based on similarity algorithms, and sorts potential drug-target interactions, which is more comprehensive and persuasive for finding effective hub targets.

ALDH3A1 was reported to be able to regulate cell proliferation and stem cell-like characteristics[23]. As a metabolic enzyme, ALDH3A1 can promote lactic acid production by regulating NAD+/NADH, promoting glycolysis, the main way of tumor energy supply, but weakening the role of OXPHOS, a relatively inefficient way in tumor cells, NAD + metabolism links energy status with adaptive cellular and organismal responses[24–27], and NAD+/NADH ratio control the balance of OXPHOS and glycolysis[28, 29], In this study, we found that β-elemene targeting ALDH3A1 by not only down-regulating its expression at the mRNA and protein levels, but also inhibiting its enzyme activity. Consequently, the suppression of ALDH3A1 by β-elemene leading to decreased the ratio of NAD+/NADH resulting in a large amount of NAD + dissociated in the cytoplasm, and the oxidized form of cellular NAD+, NADH, is critical for mitochondrial function,which was injured in cancer cells[30]. Accumulated NAD + produced negative feedback inhibition on the transformation of pyruvate to lactic acid during glycolysis, and accumulated NADH further inhibited the upstream reaction (the process catalyzed by GAPDH), resulting in down-regulation of glycolysis and decrease of NAD+/NADH ratio. More important, our in vivo metabolomics results further verified the inhibition of aerobic glycolysis and the activation of oxidative phosphorylation. The relative amount of ATP in the tumor was significantly down-regulated compared with the control group, further certifying that β-elemene can compensate for the slow OXPHOS of energy supply by inhibiting rapid aerobic glycolysis. Reduce the energy supply efficiency of tumor growth, and then inhibit the biosynthesis of DNA, inhibit tumor proliferation.

When the decreased glycolysis under β-elemene lead to energy depletion, mitochondrial function played a secondary compensatory role, resulting in up-regulation of α-KG, succinic acid, malic acid and other intermediate metabolites suppressed in tumors. The up-regulation of α-KG, the product of TCA cycle, induced the degradation of HIF-1α by hydroxylation under normoxic condition[19, 31–33]. Moreover, β-elemene down-regulates HIF-1α, which was an important transcription factor of Warburg Effect, and the process of aerobic glycolysis by down-regulating its transcribed protein GLUT1, LDHA, and PFKL, which suggests that β-elemene regulates the balance of glycolysis and OXPHOS by targeting ALDH3A1 via HIF1 α / LDHA pathway inhibition. Certainly, metabolic reprogramming also occurs in the tumor microenvironment[34–36], and the effects of drugs are often a comprehensive systemic effect. Therefore, whether β-elemene has a similar effect on the tumor microenvironment will be the focus of our future study.

In order to further verify the anti-tumor mechanism of β-elemene. In addition to applying metabolomics, we first tried to apply ^{18}FDG-micro-PET to verify the regulation of β-elemene on glucose metabolism in vivo. ^{18}FDG-PET is one of the main tools for clinical diagnosis and evaluation of drug responsibility. Taking advantage of the significant difference in glucose absorption capacity between tumor tissues and

normal tissues, ^{18}F-labeled glucose (^{18}FDG) is used to track tissues with significantly increased metabolic ability in vivo. We used this tool to evaluate the mechanism of β-elemene, which more objectively and accurately reflected the inhibitory effect of β-elemene on glucose metabolism in tumor. Simultaneously, our results also proved that in the future the efficacy of β-elemene can be effectively evaluated by PET in clinic.

5. Conclusions

In summary, we provided new evidence that β-elemene targets ALDH3A1 in NSCLC in vivo and in vitro, and found that high expression of ALDH3A1 promote the proliferation of NSCLC via interfering with the NAD+/NADH ratio, which finally causing glycolysis considerably enhanced while OXPHOS capacity significantly reduced in cancer cells. Moreover, β-elemene targeted ALDH3A1 to regulate NAD+/NADH ratio and the increased the product of TCA cycle, α-KG, to further inhibit HIF1 α / LDHA signal pathway, thus inhibiting NSCLC progression. This study demonstrated the potential of β-elemene as a front-line treatment.

Abbreviations

NSCLC
Non-small cell lung cancer
ALDH3A1
Aldehyde Dehydrogenase 3 Family Member A1
OXPHOS
oxidative phosphorylation
α-KG
α-ketoglutarate
HIF1α
Hypoxia Inducible Factor1 Subunit Alpha
GLUT1
Glucose Transporter Type 1
PFKL
Phosphofructokinase, Liver Type
LDHA
Lactate Dehydrogenase A
Sh
Short hairpin
OE
Overexpression
FITC
Fluorescein isothiocyanate

PI
Propidium iodide

Declarations

Ethics approval and consent to participate

Not appliable.

Consent for publication

Not appliable.

Availability of data and materials

The datasets generated and/or analyzed during the current study are available from the corresponding author on reasonable request.

Competing interests

The authors declare that they have no competing interests.

Funding

The study was supported by National Natural Science Foundation of China (Grant No. 81972197 and 81472193) (Xuejun Hu).

Authors' contributions

YC, YZ, XH conceived of the study, and participated in its design and coordination and helped to draft the manuscript. XL, YY, MD, KH, YD participated in the design of the ^{18}FDG-micro-PET assay and performed the statistical analysis. YC, YZ, XH, XC, YL drafted the manuscript. All authors read and approved the final manuscript.

Acknowledgements

The study was supported by National Natural Science Foundation of China (Grant No. 81972197 and 81472193). We thank Professor Yunpeng Liu from China Medical University for providing chances and great platform to get further knowledge about Network pharmacology which is the foundation of the whole study. In addition, the authors would like to acknowledge the Key Laboratory of Precision Diagnosis and Treatment of Gastrointestinal Tumors, Ministry of Education (China Medical University, Shenyang, China) for providing the space and equipment for conducting the experiments. We also thank Professor Yaming Li from China Medical University for providing ^{18}FDG micro-PET platform to finish further mechanism exploration of the study.

References

1. Smith RA, Andrews KS, Brooks D, Fedewa SA, Manassaram-Baptiste D, Saslow D, et al. Cancer screening in the United States, 2019: A review of current American Cancer Society guidelines and current issues in cancer screening. CA Cancer J Clin. 2019;
2. Siegel RL, Miller KD, Jemal A. Cancer statistics, 2019. CA Cancer J Clin. 2019;
3. Hirsch FR, Scagliotti G V., Mulshine JL, Kwon R, Curran WJ, Wu YL, et al. Lung cancer: current therapies and new targeted treatments. Lancet. 2017.
4. Tan CS, Kumarakulasinghe NB, Huang YQ, Ang YLE, Choo JRE, Goh BC, et al. Third generation EGFR TKIs: Current data and future directions. Mol. Cancer. 2018.
5. Soria JC, Ohe Y, Vansteenkiste J, Reungwetwattana T, Chewaskulyong B, Lee KH, et al. Osimertinib in untreated EGFR-Mutated advanced non-small-cell lung cancer. N Engl J Med. 2018;
6. Kanehisa M, Furumichi M, Tanabe M, Sato Y, Morishima K. KEGG: New perspectives on genomes, pathways, diseases and drugs. Nucleic Acids Res. 2017;
7. Kong Q, Ma Y, Yu J, Chen X. Predicted molecular targets and pathways for germacrone, curdione, and furanodiene in the treatment of breast cancer using a bioinformatics approach. Sci Rep [Internet]. Springer US; 2017;7:1–11. Available from: http://dx.doi.org/10.1038/s41598-017-15812-9
8. Lu JJ, Dang YY, Huang M, Xu WS, Chen XP, Wang YT. Anti-cancer properties of terpenoids isolated from Rhizoma Curcumae - A review. J. Ethnopharmacol. 2012.
9. Zhu TZ, Li XM, Luo LH, Xu YH, Cao P, Liu Y, et al. β-elemene inhibits proliferation through crosstalk between glia maturation factor β and extracellular signal-regulated kinase 1/2 and impairs drug resistance to temozolomide in glioblastoma cells. Mol Med Rep. 2014;
10. Zhang Y, Mu XD, Li EZ, Luo Y, Song N, Qu XJ, et al. The role of E3 ubiquitin ligase Cbl proteins in β-Elemene reversing multi-drug resistance of human gastric adenocarcinoma cells. Int J Mol Sci. 2013;
11. Pan Y, Wang W, Huang S, Ni W, Wei Z, Cao Y, et al. Beta-elemene inhibits breast cancer metastasis through blocking pyruvate kinase M2 dimerization and nuclear translocation. J Cell Mol Med. 2019;
12. Zhai B, Zhang N, Han X, Li Q, Zhang M, Chen X, et al. Molecular targets of β-elemene, a herbal extract used in traditional Chinese medicine, and its potential role in cancer therapy: A review. Biomed Pharmacother [Internet]. 2019;114:108812. Available from: https://linkinghub.elsevier.com/retrieve/pii/S0753332219306651
13. Yu X, Xu M, Li N, Li Z, Li H, Shao S, et al. β-elemene inhibits tumor-promoting effect of M2 macrophages in lung cancer. Biochem Biophys Res Commun. 2017;
14. Liu Z, Du J, Yan X, Zhong J, Cui L, Lin J, et al. TCMAnalyzer: A Chemo- and Bioinformatics Web Service for Analyzing Traditional Chinese Medicine. J Chem Inf Model. 2018;
15. Zhang G, Jiang X, Liu Y, Hao X, Wang Y, Yan X, et al. Therapeutic Efficiency of an External Chinese Herbal Formula of Mammary Precancerous Lesions by BATMAN-TCM Online Bioinformatics Analysis Tool and Experimental Validation. Evidence-based Complement Altern Med. 2019;
16. Hopkins AL. Network pharmacology: The next paradigm in drug discovery. Nat. Chem. Biol. 2008.

17. Chen Y, Wu J, Yan H, Cheng Y, Wang Y, Yang Y, et al. Lymecycline reverses acquired EGFR-TKI resistance in non–small-cell lung cancer by targeting GRB2. Pharmacol Res. 2020;
18. Hermans D, Gautam S, García-Cañaveras JC, Gromer D, Mitra S, Spolski R, et al. Lactate dehydrogenase inhibition synergizes with IL-21 to promote CD8+ T cell stemness and antitumor immunity. Proc Natl Acad Sci U S A. 2020;
19. MacKenzie ED, Selak MA, Tennant DA, Payne LJ, Crosby S, Frederiksen CM, et al. Cell-Permeating α-Ketoglutarate Derivatives Alleviate Pseudohypoxia in Succinate Dehydrogenase-Deficient Cells. Mol Cell Biol. 2007;
20. Liu X, Ouyang S, Yu B, Liu Y, Huang K, Gong J, et al. PharmMapper server: A web server for potential drug target identification using pharmacophore mapping approach. Nucleic Acids Res. 2010;
21. Wang X, Shen Y, Wang S, Li S, Zhang W, Liu X, et al. PharmMapper 2017 update: A web server for potential drug target identification with a comprehensive target pharmacophore database. Nucleic Acids Res. 2017;
22. Liu Z, Guo F, Wang Y, Li C, Zhang X, Li H, et al. BATMAN-TCM: A Bioinformatics Analysis Tool for Molecular mechANism of Traditional Chinese Medicine. Sci Rep. 2016;
23. Matsunaga N, Ogino T, Hara Y, Tanaka T, Koyanagi S, Ohdo S. Optimized dosing schedule based on circadian dynamics of mouse breast cancer stem cells improves the antitumor effects of aldehyde dehydrogenase inhibitor. Cancer Res. 2018;
24. Muzio G, Maggiora M, Paiuzzi E, Oraldi M, Canuto RA. Aldehyde dehydrogenases and cell proliferation. Free Radic. Biol. Med. 2012.
25. Voulgaridou GP, Kiziridou M, Mantso T, Chlichlia K, Galanis A, Koukourakis MI, et al. Aldehyde dehydrogenase 3A1 promotes multi-modality resistance and alters gene expression profile in human breast adenocarcinoma MCF-7 cells. Int J Biochem Cell Biol [Internet]. Elsevier Ltd; 2016;77:120–8. Available from: http://dx.doi.org/10.1016/j.biocel.2016.06.004
26. Zhang X, Yang XR, Sun C, Hu B, Sun YF, Huang XW, et al. Promyelocytic leukemia protein induces arsenic trioxide resistance through regulation of aldehyde dehydrogenase 3 family member A1 in hepatocellular carcinoma. Cancer Lett. 2015;
27. Wang C, Xu J, Yuan D, Bai Y, Pan Y, Zhang J, et al. Exosomes carrying ALDOA and ALDH3A1 from irradiated lung cancer cells enhance migration and invasion of recipients by accelerating glycolysis. Mol Cell Biochem. 2020;
28. Berger F, Ramírez-Hernández MH, Ziegler M. The new life of a centenarian: Signalling functions of NAD(P). Trends Biochem. Sci. 2004.
29. Cantó C, Menzies KJ, Auwerx J. NAD+ Metabolism and the Control of Energy Homeostasis: A Balancing Act between Mitochondria and the Nucleus. Cell Metab. 2015.
30. Zhang H, Ryu D, Wu Y, Gariani K, Wang X, Luan P, et al. NAD+ repletion improves mitochondrial and stem cell function and enhances life span in mice. Science (80-). 2016;
31. Semenza GL. HIF-1: upstream and downstream of cancer metabolism. Curr. Opin. Genet. Dev. 2010.

32. Jaakkola P, Mole DR, Tian YM, Wilson MI, Gielbert J, Gaskell SJ, et al. Targeting of HIF-α to the von Hippel-Lindau ubiquitylation complex by O2-regulated prolyl hydroxylation. Science (80-). 2001;
33. Xiang S, Gu H, Jin L, Thorne RF, Zhang XD, Wu M. LncRNA IDH1-AS1 links the functions of c-Myc and HIF1α via IDH1 to regulate the Warburg effect. Proc Natl Acad Sci U S A. 2018;
34. Zheng J. Energy metabolism of cancer: Glycolysis versus oxidative phosphorylation (review). Oncol. Lett. 2012.
35. Chang CH, Qiu J, O'Sullivan D, Buck MD, Noguchi T, Curtis JD, et al. Metabolic Competition in the Tumor Microenvironment Is a Driver of Cancer Progression. Cell. 2015;
36. Phan LM, Yeung SCJ, Lee MH. Cancer metabolic reprogramming: importance, main features, and potentials for precise targeted anti-cancer therapies. Cancer Biol. Med. 2014.

Tables

Table S1: The bioinformatics analysis tool BATMAN-TCM was used to search predicted targets with PubChem CID

Compound	Predicted targets[Gene Symbol]ranked according to the decreasing				Score
PubChem_CID: 6918391	KCND1	KCNA3	PRKAB1	ADH1A	80.882
	KCNA10	GAMT	KCNC3	KCNA1	
	KCNA2	TPO	CAT	KCNB1	
	ADH1B	DLG4	KCNC2	KCNC1	
	ADH1C	KCNB	KCNA5	RNASE1	
	KCND2	ALDH2	KCNA4	KCNA7	
	KCNA6	KCND3			
	GUCY1B3	GATM	KCNK4	IYD	55.444
	KCNQ1				

Figures

Figure 1

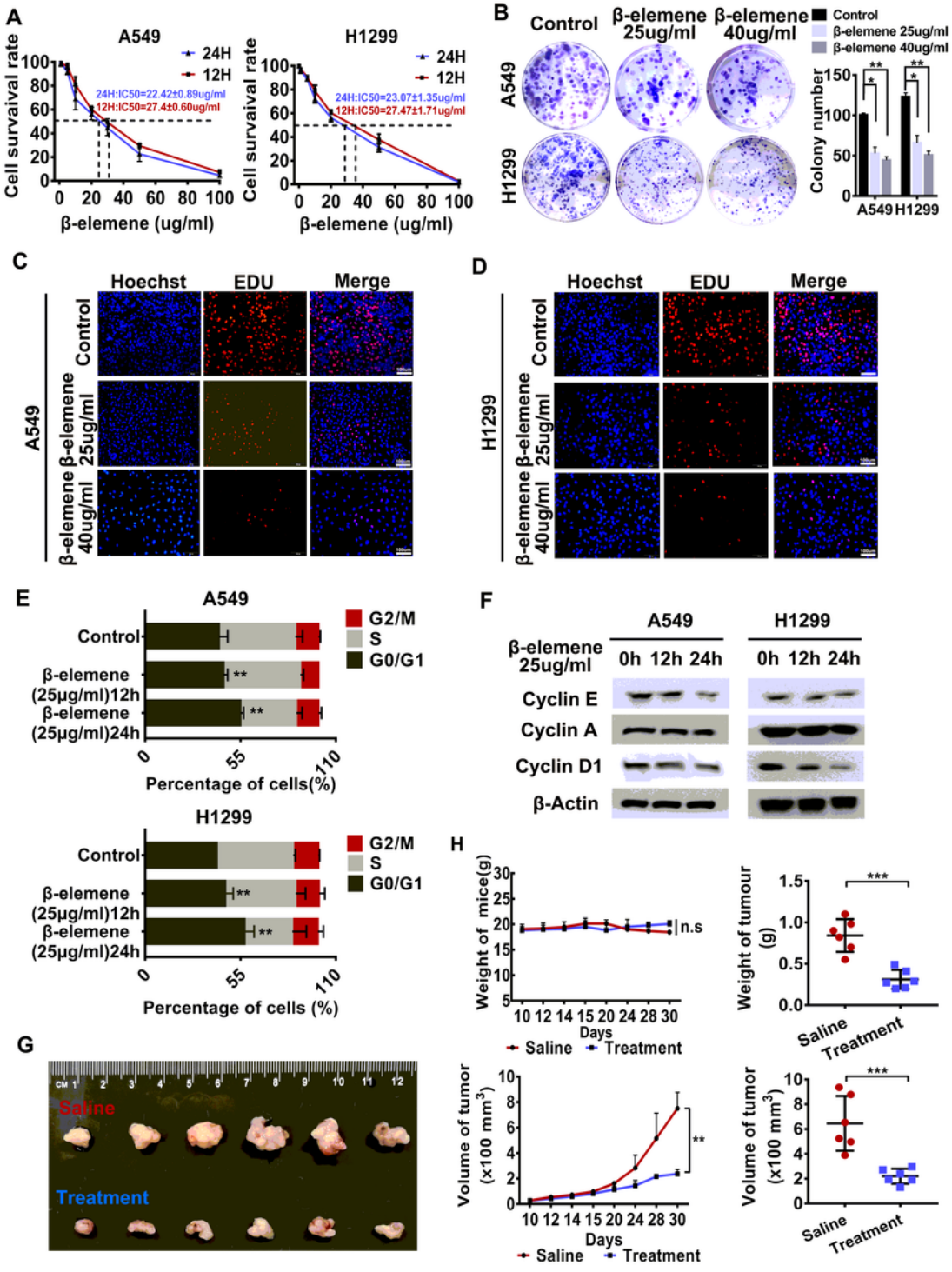

Figure 1

β-Elemene inhibited NSCLC cells proliferation by alternating the cell cycle. a. MTT assays indicating the cytotoxicity of β-elemene in NSCLC cells including A549 and H1299. b. NSCLC cells treated with high or low dose of β-elemene, followed by a colony-forming assay, and the clones were numerated. c-d. An EdU assay of two cell lines under identical conditions for 24 h, followed by sequential EdU and Hoechst staining. Hoechst 33342 (blue) represents cell nuclei and EdU (red) represents nuclei of proliferative

cells.e.Effect of the β-elemene on cell cycle distribution of A549 and H1299 cells. Data are presented as mean ± SD (n= 3, *p < 0.05). Student's t-tests were used for statistical analyses. f. Effect of β-elemene on the expression of cell cycle markers Cyclin E, Cyclin A and Cyclin D1.g. Photographs of tumors four weeks after injection with 1×107 A549 cells in 150 μL PBS. Each trial included six mice treated with PBS (150 μL by oral gavage twice daily); β-elemene (50 mg/kg by oral gavage twice daily) h. The weight and volume of the photographed tumors and mice.

Figure 2

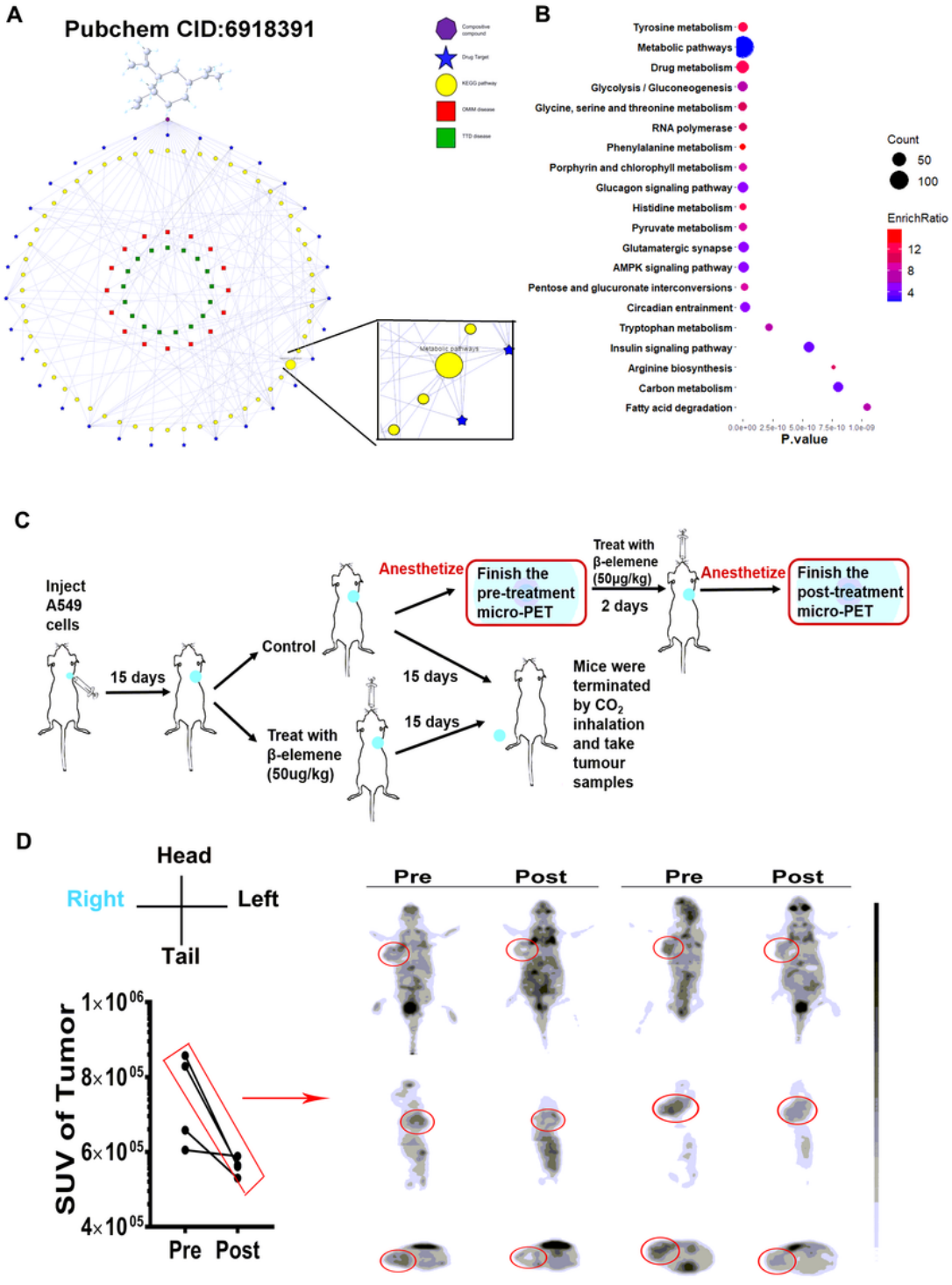

Figure 2

β-Elemene regulated metabolic reprogramming. a. Network pharmacology analysis by BATMAN-TCM. b. KEGG pathway analysis of all the target proteins in PPI. c. The diagrammatic sketch of the steps taken to build the mice model to identify the efficacy of β-elemene. d. The 18FDG micro-PET scan before and after treating with β-elemene and the SUV values of the tumors in vivo.

Figure 3

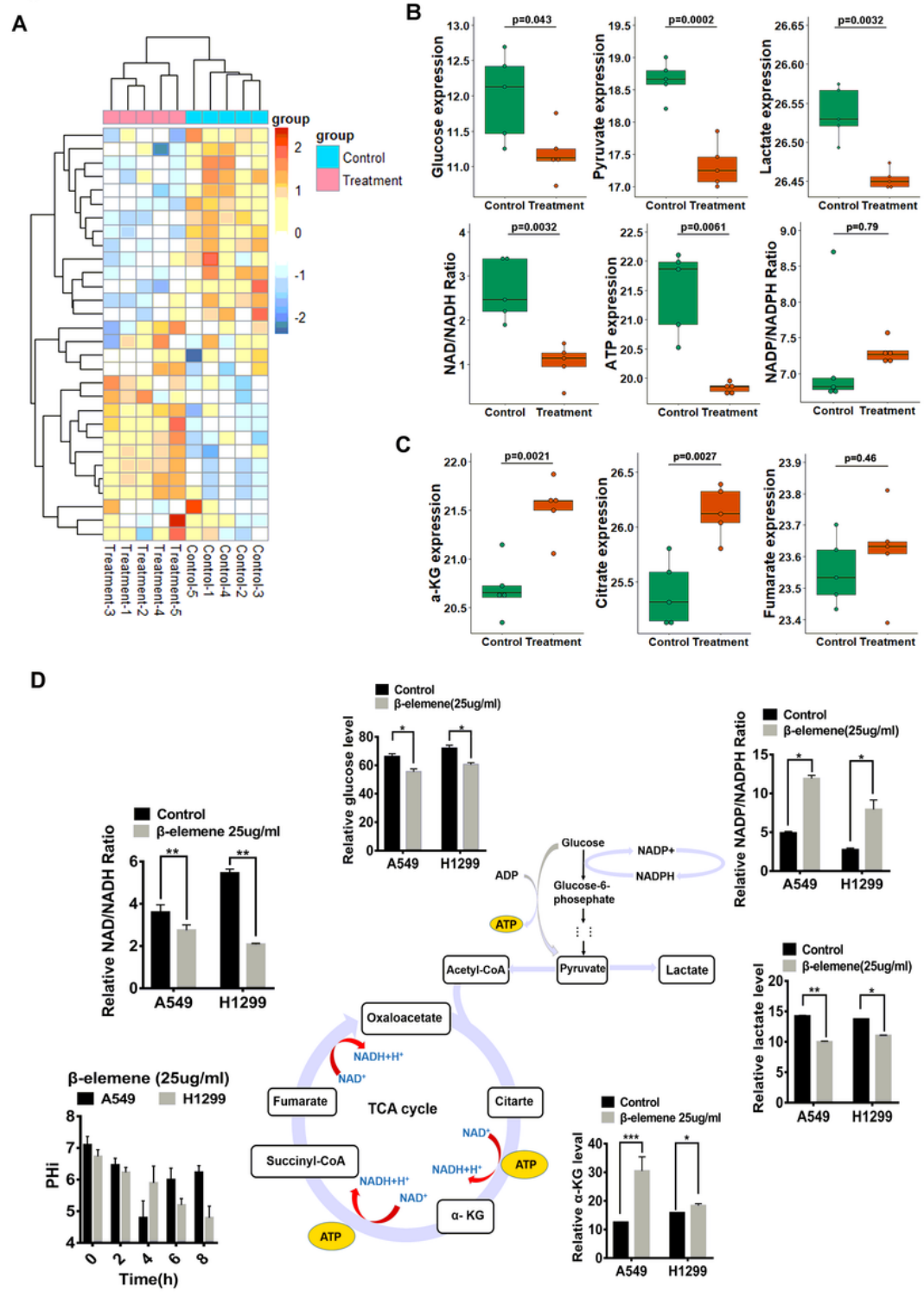

Figure 3

β-Elemene regulated the balance of glycolysis and oxidative phosphorylation.a.13C metabolite labeling and quantification of energy metabolites in the mice models. b-c. The metabolites in glycolysis and TCA cycle in tumors. d. The metabolites in glycolysis and TCA cycle in NSCLC cells.

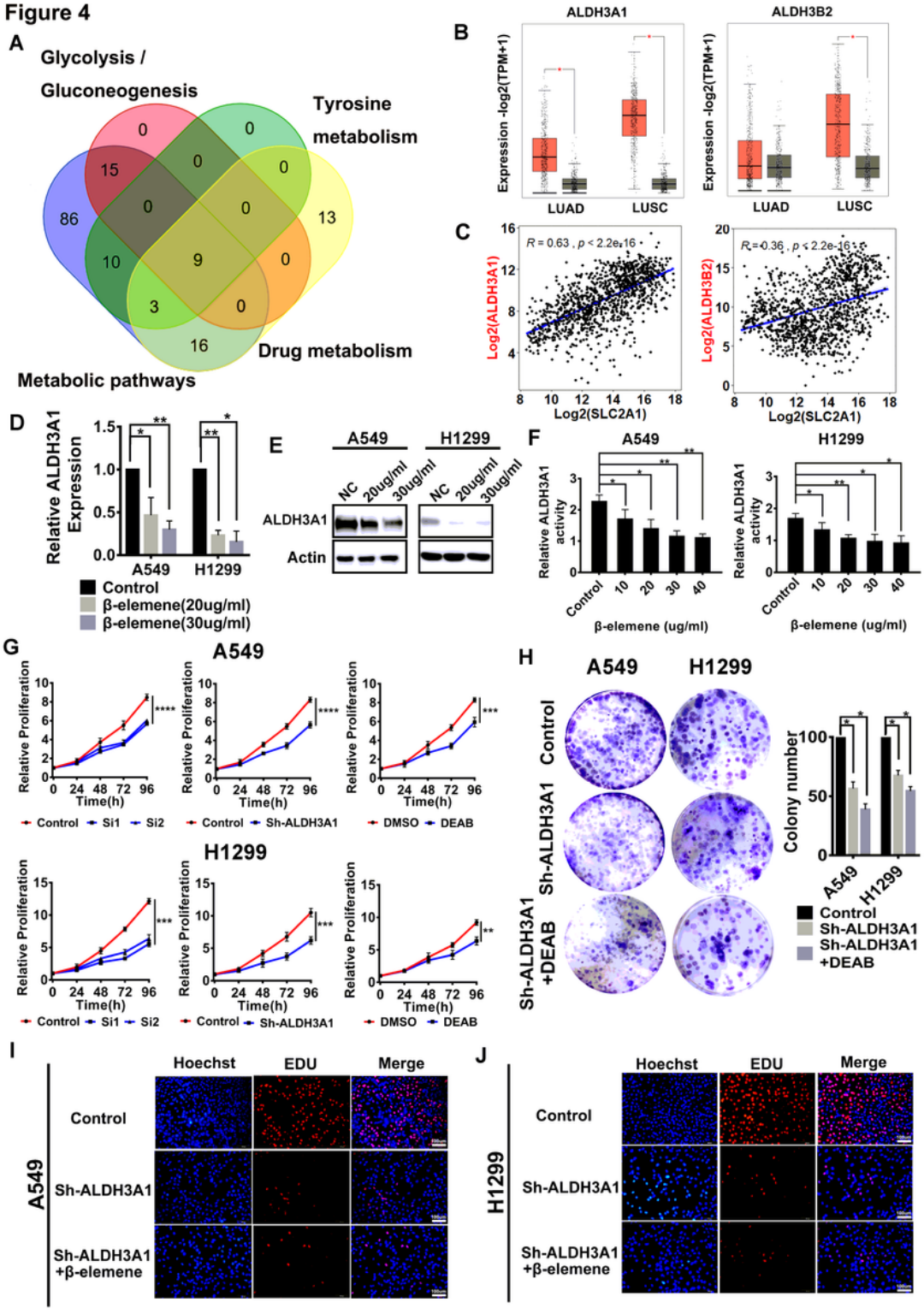

Figure 4

β-Elemene targeted ALDH3A1 to inhibit NSCLC cell proliferation a. Venn diagram of the genes in the top 4 KEGG pathways that were affected by β-elemene. b. The expression of ALDH3A1 and ALDH3B2 in NSCLC

patients. c. Correlation between hub genes of β-elemene and glycolysis related gene. d-e. Effect of β-elemene on the expression of ALDH3A1 at the RNA and protein levels. f. Effect of β-elemene on the expression of ALDH3A1. g. The viability of A549 and H1299 cells after treatment with si-ALDH3A1, Sh-ALDH3A1 or DEAB via MTT assays. h. NSCLC cells treated with Sh-ALDH3A1 and DEAB, followed by a colony-forming assay, and the clones were numerated. i-j. An EdU assay was conducted using two cell lines with Sh-ALDH3A1and β-elemene treatment.

Figure 5

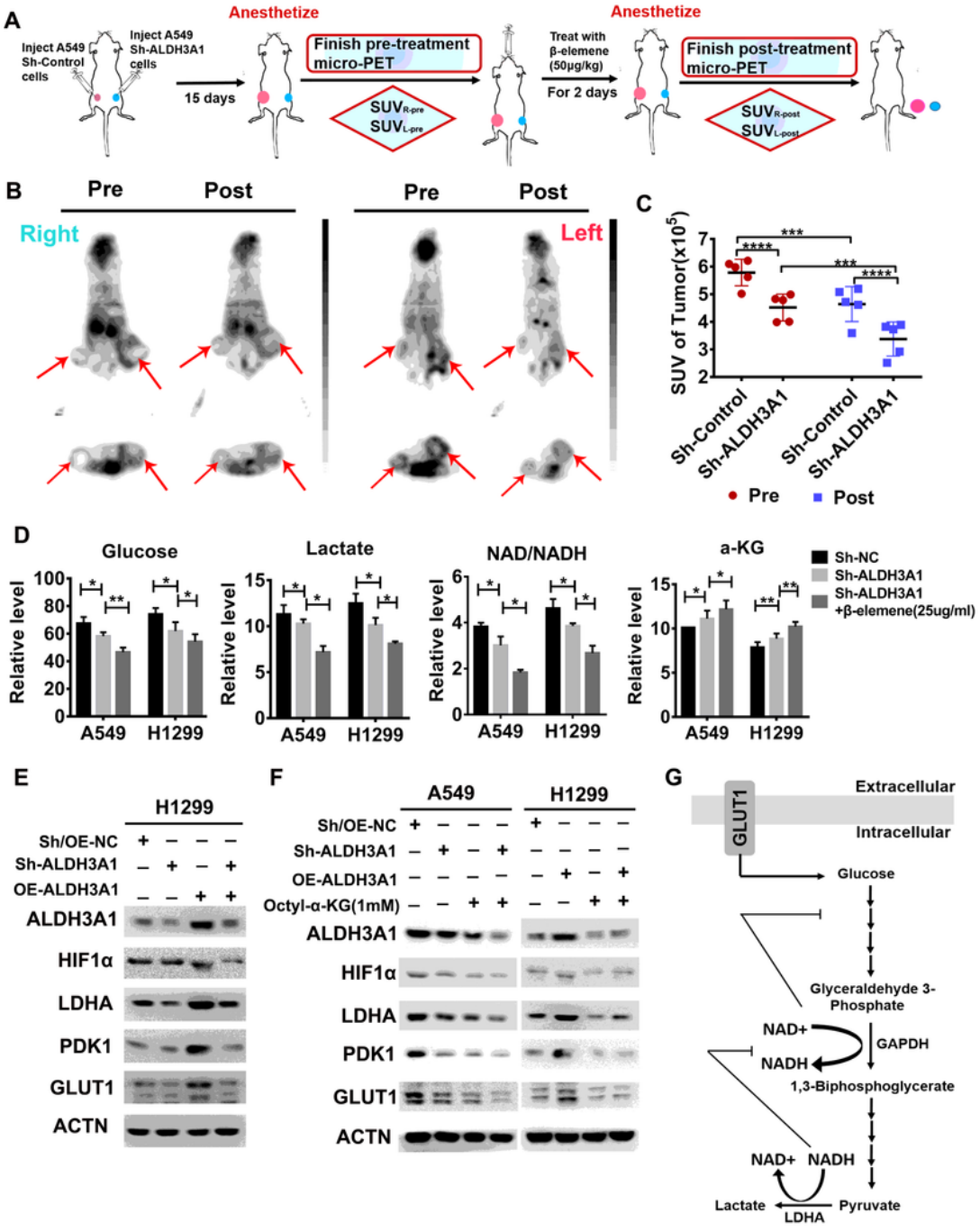

Figure 5

ALDH3A1 control HIF1α-Mediated NSCLC cell glycolysis. a. The diagrammatic sketch of the steps taken to build the mice model to identify the efficacy of β-elemene and Sh-ALDH3A1 in vivo. b. The 18FDG micro-PET scan before and after treating with β-elemene and Sh-ALDH3A1. c. the SUV values of the tumors in vivo. d. The effects of β-elemene and Sh-ALDH3A1 separately and in combination on the metabolites inglycolysis. e. Whole cell lysates from H1299 cells cointroduced with Sh-NC and Sh-ALDH3A1, OE-NC and OE-ALDH3A1. f. Whole cell lysates from A549 and H1299 cells transduced with Sh-NC and Sh-ALDH3A1, OE-NC and OE-ALDH3A1 with or without treatment with Octyl-α-KG(1mM) were subjected to Western blot analysis. g. Schematic representation of the regulation of glucose by ALDH3A1 active.

Figure 6

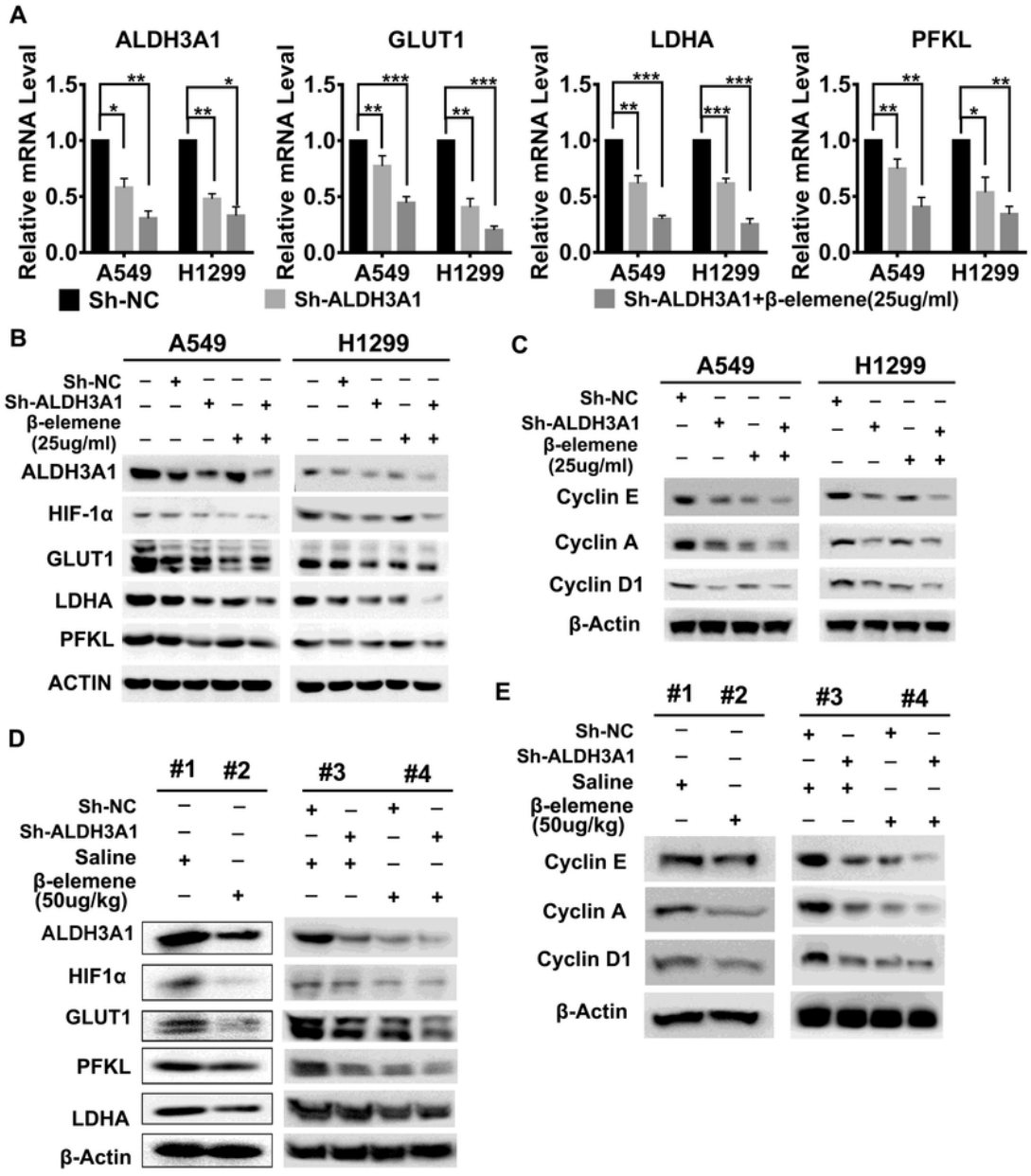

Figure 6

ALDH3A1 down-regulation by β-elemene induces HIF1α/LDHA pathway inhibited in vitro. a. The effects of combinatorial treatment with β-elemene and Sh-ALDH3A1 on the mRNA level of glycolysis genes. b-c. Whole cell lysates from A549 and H1299 cells transduced with Sh-NC and Sh-ALDH3A1with or without treatment with β-elemene(25ug/ml) were subjected to Western blot analysis. d-e. Whole cell lysates from

mice tumors transduced with Sh-NC and Sh-ALDH3A1with or without treatment with β-elemene (50ug/kg) were subjected to Western blot analysis.

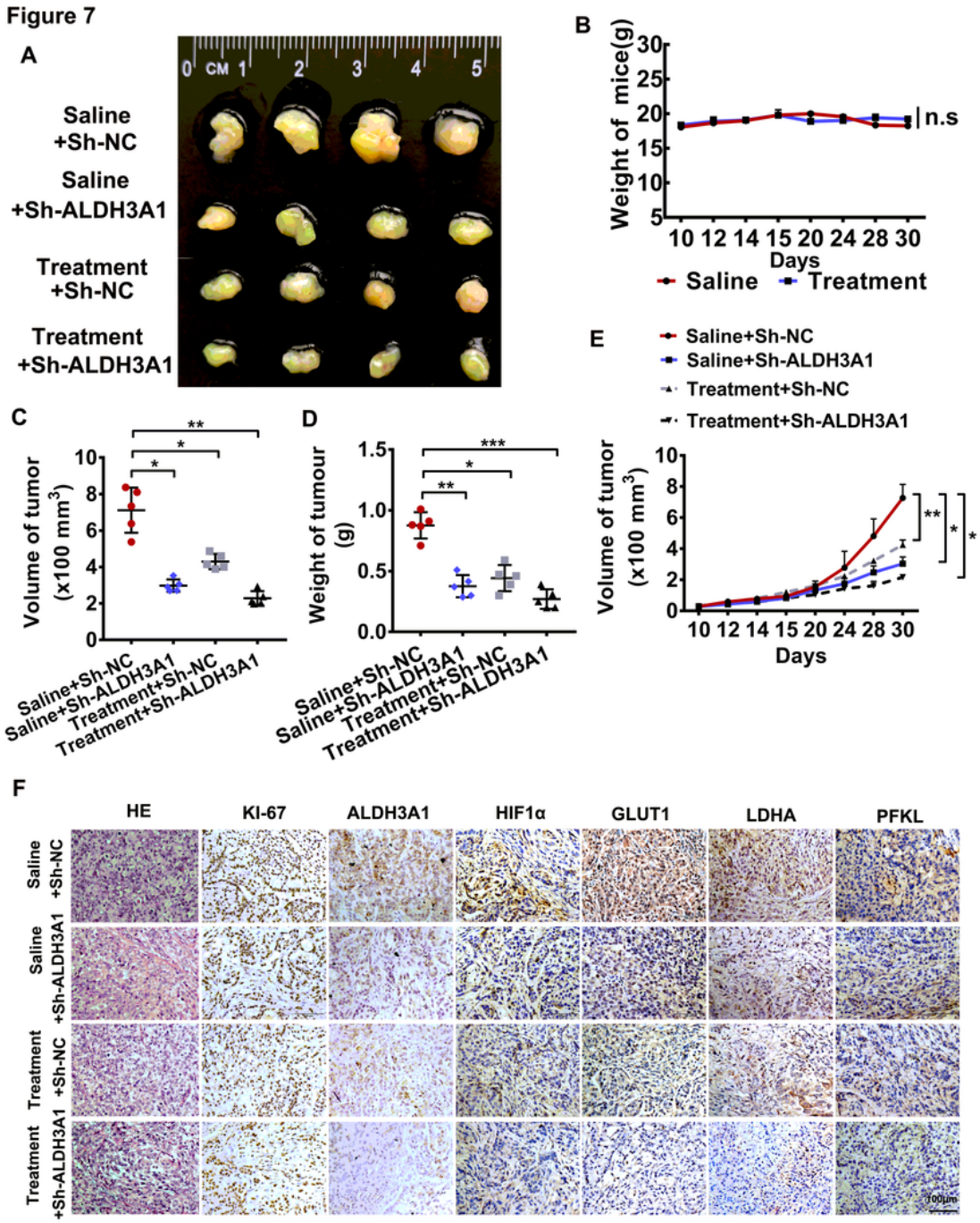

Figure 7

ALDH3A1 down-regulation by β-elemene induces HIF1α/LDHA pathway inhibited in vivo.a. Tumors four weeks after injection with 3×106 A549 cells which were transfected with Sh-NC (Left) and Sh-ALDH3A1 (Right) in 150 μL PBS. Each trial included four mice treated with PBS (150 μL by oral gavage twice daily);

β-elemene (50ug/kg by oral gavage twice daily); b. Changes in mouse weight during treatment. c-d. The weight and volume of the photographed tumors. e. Changes in tumor volume during treatment with β-elemene. f. Tumor tissue from xenografts treated for 15 days as indicated was evaluated by H&E staining and immunohistochemistry.

Supplementary Files

This is a list of supplementary files associated with this preprint. Click to download.

- FigureS1.tif
- FigureS2.tif
- FigureS3.tif
- FigureS4.tif